ORIGINAL PAPER

Assessment of glycemic response to an oral glucokinase activator in a proof of concept study: application of a semi-mechanistic, integrated glucose-insulin-glucagon model

Karen B. Schneck · Xin Zhang · Robert Bauer ·
Mats O. Karlsson · Vikram P. Sinha

Abstract A proof of concept study was conducted to investigate the safety and tolerability of a novel oral glucokinase activator, LY2599506, during multiple dose administration to healthy volunteers and subjects with Type 2 diabetes mellitus (T2DM). To analyze the study data, a previously established semi-mechanistic integrated glucose-insulin model [1–5] was extended to include characterization of glucagon dynamics. The model captured endogenous glucose and insulin dynamics, including the amplifying effects of glucose on insulin production and of insulin on glucose elimination, as well as the inhibitory influence of glucose and insulin on hepatic glucose production. The hepatic glucose production in the model was increased by glucagon and glucagon production was inhibited by elevated glucose concentrations. The contribution of exogenous factors to glycemic response, such as ingestion of carbohydrates in meals, was also included in the model. The effect of LY2599506 on glucose homeostasis in subjects with T2DM was investigated by linking a one-compartment, pharmacokinetic model to the semi-mechanistic, integrated glucose-insulin-glucagon system. Drug effects were included on pancreatic insulin secretion and hepatic glucose production. The relationships between LY2599506, glucose, insulin, and glucagon concentrations were described quantitatively and consequently, the improved understanding of the drug-response system could be used to support further clinical study planning during drug development, such as dose selection.

Introduction

Models that incorporate dynamics of physiology and pathophysiology with drug effects have been increasingly used in the development of novel anti-hyperglycemic agents over the past decade [6–9]. Mechanism-based models, also known as mechanistic models, offer an enhanced understanding of the mechanism of action of a drug and can better describe the pharmacodynamics (PD) associated with a drug [10]. Empirical models are dependent on the existing observations and can only be used to simulate in the range of observations [10]. In contrast, by incorporating physiology, mechanistic models can be used to make predictions and can be useful in guiding decisions regarding choice of patient populations, dose selection and other study design considerations encountered in drug research and development [10]. However, the application of a mechanistic model for diabetes mellitus may be impractical in certain settings. The construction of a mechanistic model often requires a large amount of clinical data for robust parameter estimation and involves an extended series of differential equations to characterize the processes in the biological system [10]. Limitations of data availability and computational resources have the potential to hinder the use of mechanistic models in the early stages

K. B. Schneck (✉) · X. Zhang · V. P. Sinha
Global PK/PD/Pharmacometrics, Eli Lilly and Company,
Lilly Corporate Center, Indianapolis, IN 46285, USA
e-mail: kschneck@lilly.com

R. Bauer
ICON Development Solutions, Ellicott City, MD, USA

M. O. Karlsson
Department of Pharmaceutical Sciences, Uppsala University,
Uppsala, Sweden

of drug development. A semi-mechanistic approach includes only selected key physiology-based processes in an attempt to reduce complexity and yet preserve the informative and predictive ability of the model [10].

The enzyme, glucokinase, is a potential drug target for anti-hyperglycemia agents due to its involvement in glucose homeostasis by contributing to the control of insulin secretion from β-cells in the pancreas and glucose conversion to glycogen in the liver [11]. A proof of concept study was conducted to investigate the safety and tolerability of a novel oral glucokinase activator, LY2599506, during multiple dose administration to healthy volunteers and subjects with T2DM. A previously developed integrated glucose-insulin model served as the starting point for describing glucose and insulin dynamics, wherein the model was able to describe the amplifying effects of glucose on insulin production and insulin on glucose elimination, as well as the inhibitory influence of glucose on hepatic glucose production [1–5]. While the previously published model was adequate for glucose provocation experiments, a counter-regulatory component describing periods of hypoglycemia was absent. Therefore, the previously published model was modified to include the influence of glucagon, such that glucose production is increased by glucagon and glucagon production is inhibited by elevated glucose concentrations. The integrated glucose-insulin model was also adapted to respond to consumed meals and was linked to a pharmacokinetic (PK) model to assess the effects of individualized LY2599506 dose amounts on glycemic response.

The goal of this analysis was to establish a model that describes the pharmacokinetic-pharmacodynamic (PK/PD) relationships that affect glucose homeostasis and the glycemic control achieved by twice daily (BID) or four times daily (QID) administration of LY2599506. The resulting semi-mechanistic, integrated glucose-insulin-glucagon model has the potential to aid future development of LY2599506 by contributing simulations to guide clinical design decisions, such as dose selection, for Phase 2 studies.

Methods

Study participants

Males or females between the ages of 21 and 70 years were included in this study. For the first study part, healthy subjects who had a body mass index (BMI) between 18.5 and 29.9 kg/m^2 and a fasting glucose <110 mg/dL were enrolled. Subjects with a clinical diagnosis of T2DM, and who were treated with diet and exercise alone or in combination with a stable dose of metformin, were enrolled for

the later parts of the study. Participants with T2DM were included if the BMI was between 18.5 and 40 kg/m^2 and hemoglobin A1c (HbA1c) was between 6.8 to 9.5 %.

The study was conducted in accordance with the ethical principles in the Declaration of Helsinki.

Study design

The study was conducted in three successive parts. The first part of the study (Part A) was a single-period, multiple-dose assessment in healthy subjects who were randomized to receive either 50 mg of LY2599506 ($n = 6$) or placebo ($n = 3$). Doses were administered prior to breakfast, lunch, dinner and bedtime (QID) for 7 days and in the morning of day 8. The second part of the study (Part B) was a dose-titration assessment in two temporally staggered cohorts of participants with T2DM. Subjects underwent titration of LY2599506 ($n = 14$) or placebo ($n = 5$) administered on a QID schedule for a total duration of 13 days. In the final part of the study (Part C), twice daily dosing (BID; at breakfast and dinner) of LY2599506 was compared to QID dosing in subjects with T2DM ($n = 13$) using a randomized two-period crossover design. The duration of LY2599506 dosing in Part C was a total of 26 days (13 days for each treatment period).

During the study, planned dose amounts of LY2599506 ranged from 50 mg to 300 mg. Doses were upwardly titrated to achieve glucose measurements at hypoglycemic thresholds or close to the limits, according to clinical judgment. A point-of-care measurement of blood glucose was obtained for immediate management decisions and for evaluation of reported symptoms of hypoglycemia. If a participant experienced blood glucose ≤60 mg/dL during Part A or B, the dose was reduced. A hypoglycemia threshold of 80 mg/dL was used for dose reductions in Part C due to the outpatient setting.

Standard meals were administered at the clinical research unit in a consistent manner for each participant. Total daily caloric requirement was calculated based on the individual's body weight, allowing approximately 30 kcal/kg distributed throughout the day as 20 % of the total daily kcal for breakfast, 30 % of kcal for lunch, 40 % kcal for dinner, and 10 % (∼200 kcal) as an evening snack. Macronutrient composition of the meals provided 55 % of the calories from carbohydrate, 30 % of the calories from fat, and 15 % of the calories from protein.

Data collection

Blood samples for determination of LY2599506 concentrations were collected at 0, 0.5, 1, 2, 3.5, 5, 7, 10, 12, 15, and 24 h after the first LY2599506 dose of the day on study days 1 and 7 in Part A, on study days 1, 3, 6, and 12 in

Part B, and on study days 1, 13, and 26 in Part C. Plasma samples were analyzed for LY2599506 concentrations (Advion BioServices Inc, Ithaca, NY, USA) using a validated liquid chromatography/electrospray ionization-tandem mass spectrometry (LC/MS/MS) method to generate a linear response over the concentration range of 0.1 to 250 ng/mL.

Venous blood samples for glucose were collected at 0, 1, 2, 3.5, and 5 h after meals (breakfast, lunch, and dinner) and 4.5 h after the snack provided at bedtime on the baseline day and study days 3, 6, and 12 in Part B and on the baseline day and study days 13 and 26 in Part C. The venous blood samples collected for insulin and glucagon concentrations were obtained at 0, 1, 2, 3.5, and 5 h after the morning meal (breakfast) on the baseline day and study days 3, 6, and 12 in Part B. Sampling for insulin and glucagon occurred at 0, 1, 2, 3.5, 5 h after all daytime meals (breakfast, lunch, and dinner) on the baseline day and study days 13 and 26 in Part C. Glucose, insulin, and glucagon were assayed using standard, validated methods at a central laboratory.

LY2599506 concentration data collected from healthy subjects (Part A) and subjects with T2DM (Part B and C) were included in the PK analysis. Glucose, insulin, and glucagon data collected from subjects with T2DM (Parts B and C) were included in the PK/PD analysis.

Model description

Integrated glucose-insulin model

The glucose and insulin scheme used in this analysis was based on the integrated glucose-insulin model developed by Jauslin et al. and Silber et al., which has been discussed in detail previously [1–5]. The key components of the glucose and insulin feedback system are briefly described below.

In the glucose sub-model, the introduction of exogenous glucose into the system is represented by an absorption rate constant (k_{abs}) between the glucose absorption compartment and the central glucose distribution compartment. Systemic glucose is distributed into a central and a peripheral distribution space. Movement of glucose in the system, both elimination from the system and movement between compartments (Q), is parameterized in terms of clearance. The removal of glucose from the system is accomplished by two pathways: clearance of glucose independent from the influence of insulin (CL_G) and clearance of glucose affected by insulin (CL_{GI}), (see Fig. 1).

The insulin sub-model is comprised of a baseline secretion of insulin and clearance of insulin from a central insulin compartment (CL_I), (see Fig. 1). The secretion of insulin is stimulated by elevated glucose amounts and is also characterized by a circadian rhythm [4].

Delays in the effects of glucose and insulin were included in the model by the use of first-order rate constants between the central compartments and the effect compartments (Fig. 1).

The contribution of meal intake to the dynamics of glucose was incorporated into the model by considering the macronutrient composition of the meals. Carbohydrate from meals in units of kcal was converted to grams of glucose input by assuming that 1 kcal of carbohydrate was equivalent to 0.25 grams of glucose.

Certain physiologically related parameters for glucose and insulin, such as volumes of distribution, were fixed to previously published values [4] in order to reduce the computational intensity of the model (Table 3). The parameters describing the circadian rhythmic pattern of insulin secretion (MA, MW, and MT_{max}) were set to fixed values since the deficiency of nighttime sampling for insulin in the current study did not permit parameter estimation (Table 3).

Inter-individual variability for parameters was estimated using a log-normal distribution. Residual error was estimated for glucose and insulin separately using a proportional error structure.

Glucagon regulation

The glucose-insulin scheme described above was extended by incorporating a glucagon component. The glucagon sub-model included a central compartment and glucagon clearance (CL_{GN}). Baseline glucagon secretion (Eq. 1), the inhibitory influence of glucose (Eq. 2) and insulin (Eq. 3), and the stimulatory influence of ingested exogenous protein on glucagon secretion (Eq. 4) were combined in a differential equation to describe glucagon dynamics (Eq. 6), (see Fig. 1). Protein content in meals was converted from kcal to grams similar to the approach used for carbohydrate to glucose conversion. The absorption rate of protein was assumed to equal the absorption rate of glucose in the glucose sub-model (k_{abs}). An effect compartment was utilized to represent a delayed effect of glucagon within the system. Residual error was estimated for glucagon using a proportional error structure.

$$GN_{PROD,0} = GN_{SS} \cdot CL_{GN} \tag{1}$$

$$E_{glucose} = (G_E \ / \ G_{SS})^{-NPRG} \tag{2}$$

$$E_{insulin} = (I_E \ / \ I_{SS})^{-NPRI} \tag{3}$$

$$E_{protein} = 1 + (GSLP \cdot A_{protein}) \tag{4}$$

$$k_{GN} = CL_{GN}/V_{GN} \tag{5}$$

$$\frac{dGNc}{dt} = (GN_{PROD,0} \cdot E_{glucose} \cdot E_{insulin} \cdot E_{protein}) - (k_{GN} \cdot GN_c) \tag{6}$$

Fig. 1 Schematic representation of the model. *Full arrows* indicate flows, *broken arrows* indicate control mechanisms, *dashed lines with triangle endpoints* denote stimulating effects, *dashed lines with circle endpoints* denote inhibitory effects. Refer to Table 1, Table 3 and Eq. 7 for abbreviations
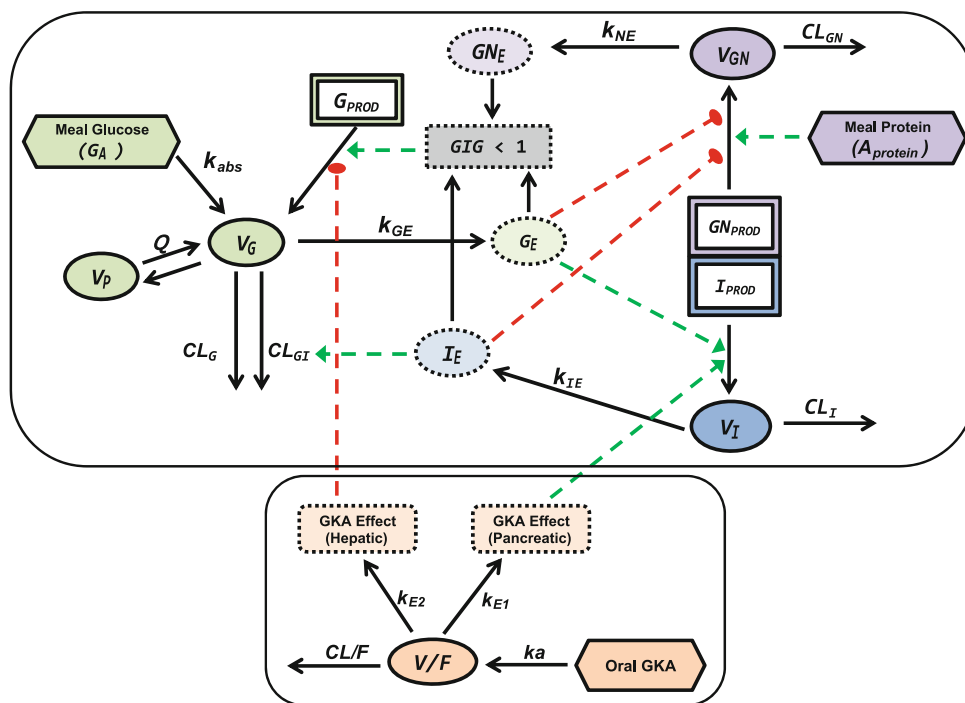
where $GN_{prod,0}$ is baseline glucagon production, GN_{SS} is glucagon concentration at steady-state, CL_{GN} is the glucagon clearance, $E_{glucose}$ is the inhibitory effect of glucose on glucagon production, G_E is the glucose effect compartment concentration, G_{SS} is the glucose concentration at steady-state, NPRG is the negative power coefficient describing the relationship between effect on glucagon production and glucose amount, $E_{insulin}$ is the inhibitory effect of insulin on glucagon production, I_E is the insulin effect compartment concentration, I_{SS} is the insulin concentration at steady-state, NPRI is the negative power coefficient describing the relationship between effect on glucagon production and insulin amount, $E_{protein}$ is the stimulatory effect of protein on glucagon production, and GSLP is the slope coefficient describing the relationship between the effect on glucagon production and protein amount ingested with a meal ($A_{protein}$), k_{GN} is the glucagon elimination rate constant, and V_{GN} is the volume of distribution of glucagon.

A stimulatory effect on hepatic glucose production was captured by a factor termed "GIG Index", which represents the composite effect of glucose, insulin and glucagon concentrations (Eq. 7).

$$GIG\ Index = (G_E\ /\ G_{ss}) \cdot (I_E\ /\ I_{ss}) \cdot (GN_{ss}\ /\ GN_E) \qquad (7)$$

where, G_E is the glucose amount in the glucose effect compartment, G_{SS} is the glucose concentration at steady-state, I_E is the insulin amount in the insulin effect compartment, I_{ss} is the insulin concentration at steady-state,

GN_E is the glucagon effect compartment concentration, and GN_{SS} is steady-state glucagon concentration.

The GIG index was then related to a fold effect on baseline hepatic glucose output (Eq. 8, Fig. 2).

$$G_{PROD,total} = G_{PROD,0} \cdot GIG^{-GPRG} \qquad (8)$$

where, $G_{PROD,total}$ is total glucose production, $G_{PROD,0}$ is basal glucose production, and GPRG is the effect of glucagon on glucose.

Initially, the integrated glucose-insulin-glucagon model was applied to data in the absence of LY2599506, that is, data collected at baseline prior to drug administration and from subjects given placebo, in order to assess the integrity of the glucose-insulin-glucagon model.

Pharmacokinetics and drug effect

The plasma LY2599506 concentration data from healthy subjects and subjects with T2DM were characterized by a one-compartment PK model parameterized in terms of absorption rate constant (ka), apparent plasma clearance (CL/F), and apparent volume of distribution (V/F). The potential effects of subject characteristics, such as age, body weight, body mass index (BMI), creatinine clearance, gender, and disease status (healthy subjects versus subjects with T2DM), on LY2599506 PK were examined. Inter-individual variability was included on ka, CL/F, and V/F according to a log-normal distribution of individual parameters. Residual error was characterized with a proportional error model.
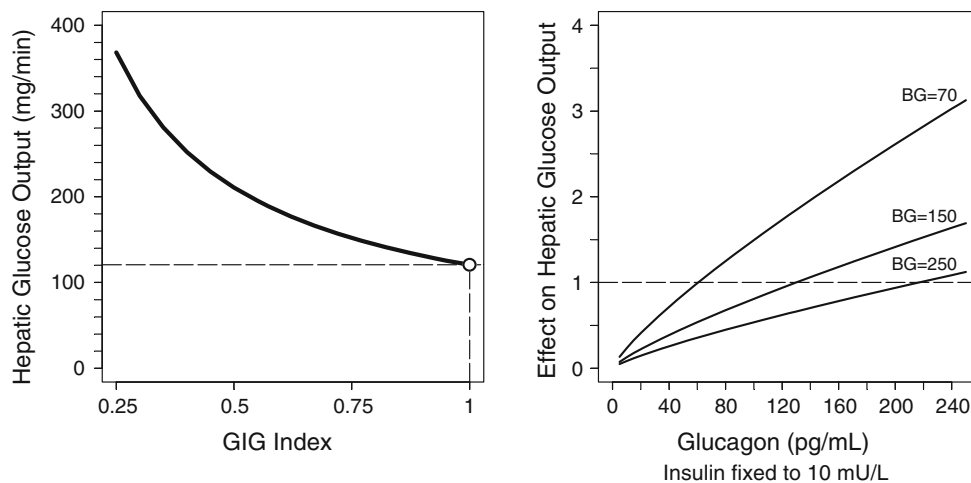
Fig. 2 Effect of glucagon on hepatic glucose output. *Left*: glucose, insulin, and glucagon concentrations were treated as a composite factor, Glucose-Insulin-Glucagon (GIG) index (Eq. 7), and were linked to the hepatic glucose output in the model (Eq. 8), where GIG = 1 corresponds to steady-state and GIG < 1 results in increased hepatic glucose output. *Right*: the magnitude of the amplifying fold-effect of glucagon on hepatic glucose output (Eq. 2) was dependent on concurrent glucose and insulin concentrations. BG, blood glucose in mg/dL

The PK model of LY2599506 was integrated with the glucose-insulin-glucagon model by employing the "sequential" approach [12, 13], wherein the PK of individuals was estimated prior to the fitting of PK/PD parameters. The relationship between LY2599506 concentration and glycemic control was investigated by including parameters for the effect of LY2599506 on insulin secretion and glucose production. The model was structured to have circulating LY2599506 in the body enter a biophase compartment, which represented the drug concentration at the site of action [14]. Each considered site of action (i.e. liver or pancreas) had an estimated rate constant (k_{E1}, k_{E2}) for drug elimination from the biophase compartment and the rate of elimination was assumed to equal the rate of entry. Various linear and nonlinear relationships (Eqs. 8, 9, and 10) between the PD and biophase concentration were explored and the most stable parameterization based on biological feasibility was selected. The influence of LY2599506 was assessed on each potential physiological site (i.e. liver or pancreas) separately and concurrently.

The primary general structures explored were as follows:

$$DE = x \cdot CE + 1 \tag{9}$$

$$DE = (1 + CE)^x \tag{10}$$

$$DE = \frac{(E_{\text{Max}} \cdot CE^x)}{(EC_{50} + CE)^x} \tag{11}$$

where DE is drug effect, CE is the LY2599506 concentration in the biophase, x represents either a slope or power coefficient, E_{max} is the maximum effect, and EC_{50} is the concentration related to 50 % of maximal effect.

Model implementation

Models were implemented using nonlinear mixed effects modeling in NONMEM, version 7.2 software [15]. The PK analysis was conducted using the first order conditional estimation (FOCE) method with interaction. The Expectation Maximization (EM) estimation method known as Monte Carlo Importance Sampling assisted by Mode A Posteriori (IMPMAP) and the differential equation solver ADVAN13 were used to execute the PK/PD model [15]. To optimize computational efficiency, parallel computing was used to run NONMEM [15]. Objective function evaluations of individual subjects were split among 4–6 CPUs on a Linux networked cluster of computers, which allowed for a reduced run time for the PK/PD model. Tabulations and plots summarizing results were produced in Spotfire S-Plus, version 8.2 (TIBCO Software Inc, Palo Alto, CA).

Model selection and evaluation

Model selection was based on goodness-of-fit plots, the plausibility of the physiological system, and the objective function value provided by NONMEM. Goodness-of-fit plots such as observed values (DV) versus population predictions (PRED), DV versus individual predictions (IPRED), and population and individual weighted residual errors versus time or versus concentrations were used for graphic assessment of the quality of the model fit. A difference in the objective function value in hierarchical models of at least $6.635 (\alpha = 0.01)$ for PK models and $10.828 (\alpha = 0.001)$ for PK/PD models was considered significant.

The predictive performance of the model was assessed by applying a visual predictive check [16]. For the evaluation of the final model, 100 data sets were simulated in NONMEM. The median and the 90 % prediction intervals of the individual concentration–time profiles of glucose, insulin, and glucagon were superimposed on the respective observed data. To assess the reliability of the standard errors estimated, the Markov Chain Monte Carlo Bayesian Analysis method (BAYES) in NONMEM was applied to generate 1000 sets of probable population parameters [15] and the median, 5th and 95th percentiles of the estimated population parameters were calculated.

Results

Demographics

A total of 41 subjects, 27 male and 14 female, between the ages of 28 and 69 years, inclusive, participated in this study. With the exception of one subject, all subjects were categorized as Caucasian. The average duration of T2DM in the subjects was approximately 7 years (range 1–18 years). The mean baseline HbA1c of subjects with T2DM was 7.4 % (range 6.5–8.7 %). Approximately 80 % of subjects with T2DM were treated with stable doses of metformin. The subjects with T2DM in Part B (9 females/10 males) had a mean (range) age, BMI, and HbA1C of 57 (37–69), 30 (20–34) and 7.4 % (6.7–9.1 %). The subjects with T2DM in Part C (3 females/10 males) had a mean (range) age, BMI, and HbA1C of 57 years (48–69 years), 31 kg/m^2 (24–37 kg/m^2) (6.7–8.7 %). The Cockcroft-Gault creatinine clearances of all study participants were greater than 60 mL/min.

At the end of the treatment period for subjects with T2DM in Part B, the mean (range) of the total daily dose of LY2599506 was 500 mg (50–1100 mg). In Part C, the mean (range) of the total daily dose of LY2599506 for subjects with T2DM was 220 mg (60–530 mg) for subjects on QID dosing schedule and 130 mg (40–200 mg) for subjects on BID dosing schedule.

On average, daily caloric consumption was 2620 kcal (range: 2090–3160 kcal) in Part B and 2800 kcal (range: 2130–3170 kcal) in Part C. Carbohydrate intake ranged from 20.7 grams to 177 grams and 10.5 grams to 177 grams in Parts B and C, respectively. The range of protein amounts from meals varied from 7 to 50.7 grams in Part B and 3.1 to 50 grams in Part C. The observed values for consumed carbohydrate and protein in each individual were used as the inputs into the integrated glucose-insulin-glucagon model.

Placebo model

The appropriateness of the integrated glucose-insulin-glucagon model for the evaluation of data from subjects with T2DM was first assessed in the absence of LY2599506 by using the data collected at baseline (prior to drug treatment) and for all days when subjects were given placebo. Published values for select fixed and random effects [4] were applied to the model (Table 3) and allowed for adequate characterization of the glucose, insulin, and glucagon dynamics as demonstrated by the concordance of the prediction intervals from the visual predictive check with the observed values at baseline (Fig. 3). The hepatic glucose production at steady-state ($G_{PROD,0}$) for subjects with T2DM in this study had a mean population value of 120 mg/min (Fig. 2) with estimates for individuals ranging between 90 and 220 mg/min (0.9–2.4 mg/kg/min). The hepatic glucose output predicted by the model was in alignment with other studies [17–20].

Drug effects

The final model for the system describing LY2599506 concentration, glucose, insulin, and glucagon is depicted in Fig. 1.

Plasma LY2599506 concentrations in healthy subjects and patients with T2DM were adequately described by a one-compartment PK model. The mean population values for ka, CL/F, V/F, time of observed maximum concentration (t_{max}), half-life ($t_{1/2}$), and accumulation index (AI) are summarized in Table 1. The model estimates of ka, CL/F and V/F, following oral administration of LY2599506, were 1.44 h^{-1}, 15.6 L/h, and 188 L, respectively. LY2599506 plasma concentration peaked around 2.3 h (range 1–4.3 h) following administration of the drug. The mean $t_{1/2}$ was 8.3 h (range 3.7–19 h), which equated to an average accumulation (AI) of approximately 2.7 following QID dosing.

No statistically significant effect of body weight, BMI, creatinine clearance, gender, or disease status (healthy subjects versus subjects with T2DM) on LY2599506 PK parameters was noted. Inclusion of age as a covariate on CL/F reduced inter-individual variability on this parameter from 47 % to 36 %. Based on this exploratory model, CL/F was inversely related to age. The PK model predicted that a subject who was 57 years old had a CL/F approximately half that of a subject who was 30 years old (16 L/h vs. 30 L/h, respectively, see Table 1). A simulation of plasma LY2599506 concentration–time profiles from subjects treated with LY2599506 is depicted in Fig. 4.

Following QID administration of LY2599506 for up to 13 days in subjects with T2DM in Part B, there was a significant reduction in the fasting plasma glucose (−34 mg/dL on Day 3, and −47 mg/dL on Day 6 and Day 12). A considerable effect of LY2599506 on time-matched, baseline-corrected postprandial glucose concentrations was also observed, ranging from ∼50–80 mg/dL after each the three
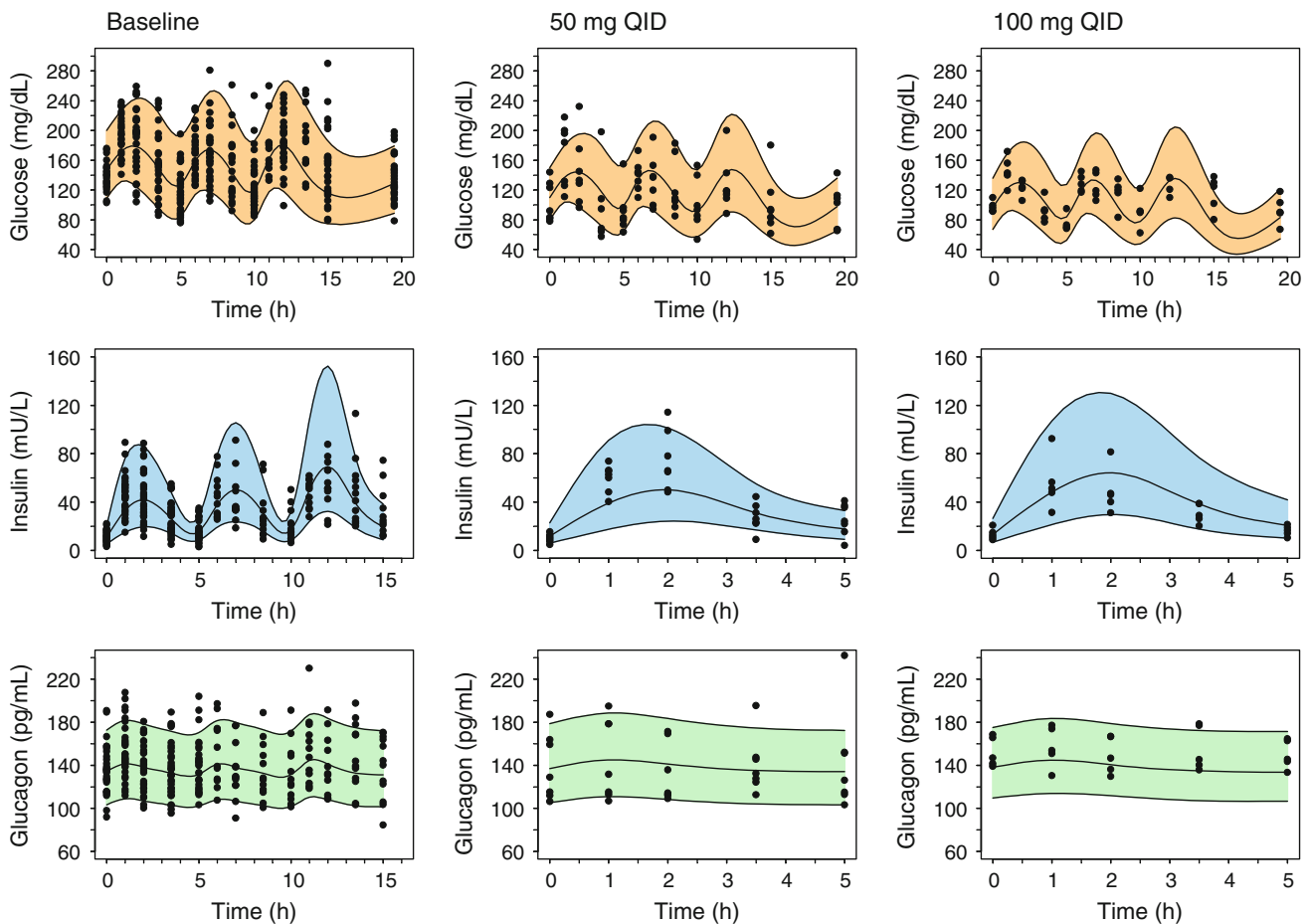
Fig. 3 Visual predictive check of glucose, insulin, and glucagon. Observations in the original data set are plotted as points. Data from Parts B and C are included in the baseline plots while LY2599506 treatment plots were restricted to 50 mg and 100 mg QID dosing in Part B for clarity purposes. One hundred data sets were simulated. The *black lines* show the median, 5th and 95th percentiles of the simulated individual predictions. Meals were given at times 0, 5, 10, and 15 h after the first dose of the day

main meals on Days 6 and 12 in Part B and from ∼25–40 mg/dL on Days 13 and 26 in Part C. The onset of significant effects of LY2599506 on glucose appeared within 2–3 days. On Day 6, near-to-maximum glucose normalization was achieved (Fig. 5). The changes in fasting glucose following BID vs. QID dosing of LY2599506 (Part C) were comparable (Fig. 6), with QID dosing offering slightly better glucose control than BID dosing (−28 and −18 mg/dL following QID and BID dosing of LY2599506 for 13 days, respectively). For a dose in Part C, steady-state glycemic response was achieved approximately three days following initial dosing. Overall, no significant changes in glucagon (Figs. 5, 6) or GLP-1 were observed.

The PK/PD model was run on the data from baseline and treatment days for both placebo and LY2599506 treated subjects with T2DM and the objective function value (OFV; −2·log(likelihood)) was set as the reference (Table 2). The effect of LY2599506 on insulin secretion was best described by a linear stimulatory relationship with the biophase LY2599506 concentration with a positive slope (DIPR), (Eq. 9). The relationship between LY2599506 and glucose production (DE$_{glucose}$) was found to improve the model fit when structured to be inhibitory with a negative power value (−DGPR), (Eq. 10). Incorporation of a drug effect parameter on insulin secretion and on hepatic glucose production resulted in a decrease in OFV compared to the reference OFV when effects were tested separately and included simultaneously (Table 2). Addition of a drug effect parameter on glucagon production was investigated and was deemed to have no detectable statistical influence on model predictions (no significant decrease in OFV was noted) and had no impact on biological plausibility. Estimated parameter values for the model retaining a drug effect on insulin secretion and hepatic glucose production are shown in Table 3.

Model evaluation

Diagnostic plots for the evaluation of the quality of the model fit illustrate that the model described the data

Table 1 LY2599506 pharmacokinetics

Parameter		Population mean	SEE (%)[a]
Absorption rate constant (ka)	(h^{-1})	1.44	16
Apparent clearance (CL/F)[b]	(L/h)	15.6	9
Apparent volume of distribution (V/F)	(L)	188	5
Time of maximum concentration (t_{max})	(h)	2.31	–[c]
Half-life ($t_{1/2}$)	(h)	8.30	–[c]
Accumulation index (AI)[d]		2.71	–[c]
Inter-individual variability (IIV)			
IIV–ka	(%)	74	28
IIV –CL/F	(%)	47	22
IIV –V/F	(%)	24	26
Residual Error			
Proportional	(%)	33	21

[a] Standard error of the estimate

[b] For an individual subject, $CL/F = 15.6 \cdot (1 + (age - 57) \cdot -0.0347)$

[c] Parameter was not estimated

[d] AI is estimated by $1/(1 - \exp(-k \cdot \tau))$ (where $k = 0.693/t_{1/2}$, τ = dosing interval assuming QID dosing)

adequately (Fig. 7). Endogenous (hepatic glucose production and insulin secretion) and exogenous (ingested meals and the administration of LY2599506) influences on the glucose-insulin system were sufficiently handled by the model, as indicated by the satisfactory appearance of the predictive check figures (Fig. 3). The medians of the simulated individual concentration–time profiles and the 5th and 95th percentiles around them are plotted over the observed profiles of glucose and insulin during baseline and treatment with LY2599506 (Days 3, 6, and 12). This visual check suggests that 90 % of the observations lie within the predictive interval. The results of the Bayesian

simulations are summarized in Table 3 and also support the ability of the model to produce predictions with fidelity. Representative profiles (Fig. 8) indicate that the model adequately predicts glucose response following individualized LY2599506 dosing and based on varying calories consumed by subjects.

Discussion

The semi-mechanistic modeling approach was a practical tool to enhance the learning gained from a proof-of-concept clinical study during early development of LY2599506, a novel oral anti-hyperglycemic agent.

The pharmacologic effects of LY2599506 on glucose regulation were clearly demonstrated and were generally consistent with the results observed after single doses [21, 22]. Glycemic control was maintained over the duration of the study and doses were increased in subjects if they did not encounter hypoglycemia at lower doses. The glucose profile in subjects with T2DM during treatment with LY2599506 was notable for a consistent reduction in both fasting and postprandial glucose values. Prandial glucose excursion (from pre-meal baseline) did not appear to be significantly affected by the dose amount of LY2599506. The contrast of BID versus QID dosing in Part C was intended to assess the PK/PD of continuous drug exposure over the 24-hour dosing interval (QID dosing) compared to the BID dosing profile. The total daily dose was lower under BID conditions (40–200 mg) compared to QID conditions (60–530 mg). This observation suggests that the maximum BID dose is limited by hypoglycemia in the post-breakfast and post-dinner periods, and that BID dosing cannot achieve sustained high concentrations of drug exposure during afternoon and nocturnal periods. In Part C, at the doses achieved, QID dosing appeared to provide greater glucose lowering during the afternoon compared to BID dosing.

Fig. 4 LY2599506 pharmacokinetic profile. The *line* shows the prediction for population median and the shaded area represents the 90th prediction interval for dose-normalized concentrations following LY2599506 administered QID on study days 1 and 3. Observations are dose-normalized concentrations from subjects administered either 50 mg (*empty circle*) or 100 mg (*empty triangle*)
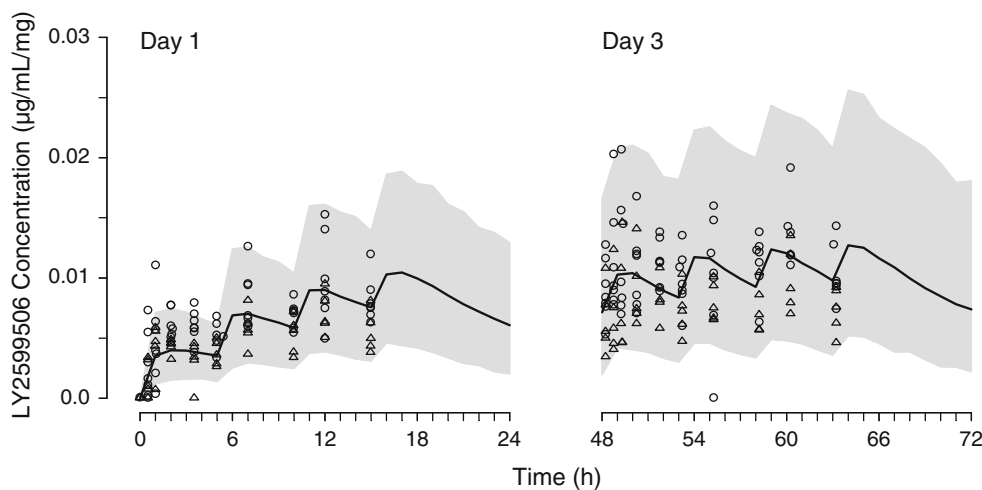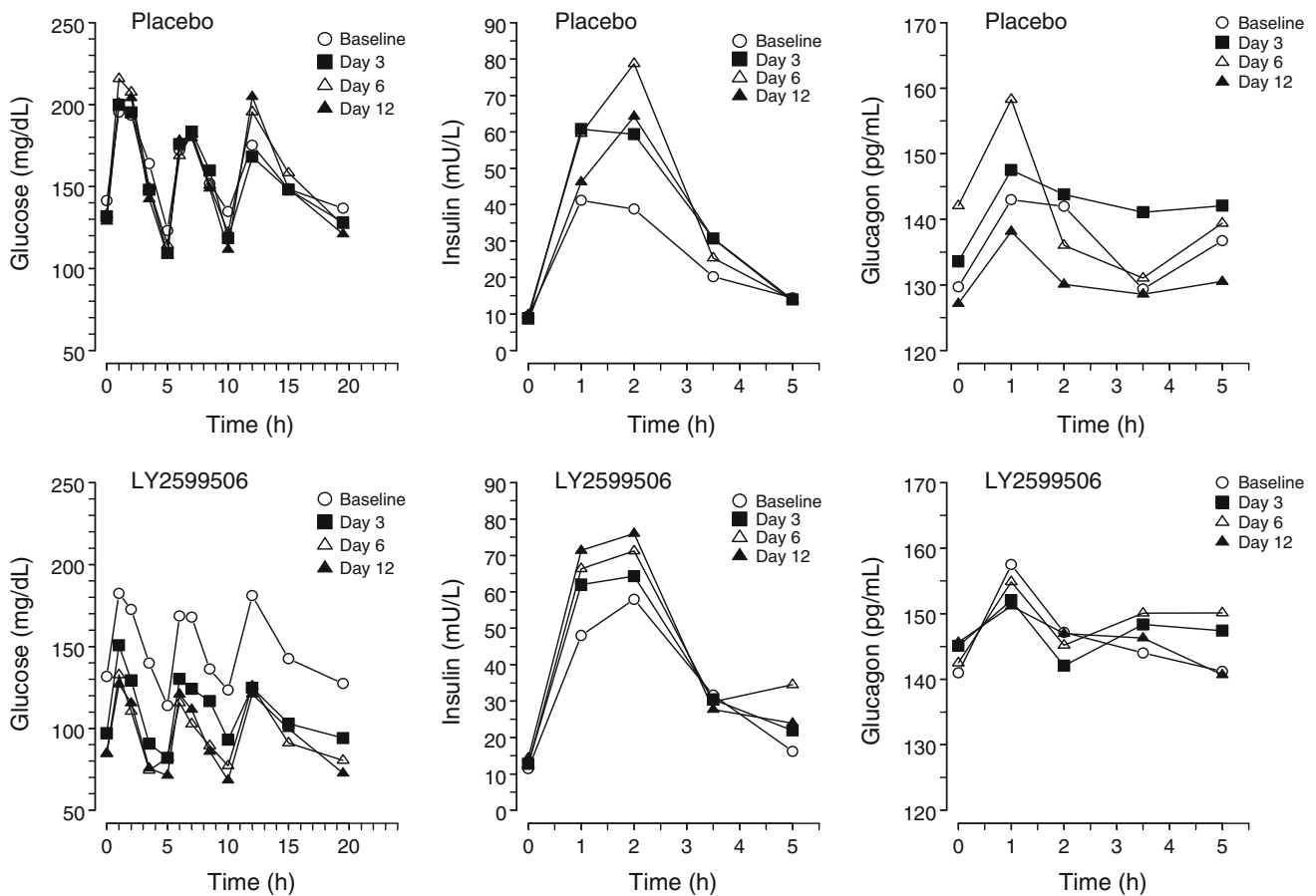
Fig. 5 Mean observed glucose, insulin, and glucagon profiles for Part B. Baseline and study days 3, 6, and 12 for subjects with T2DM administered placebo (*first row*) and LY2599506 (*second row*)
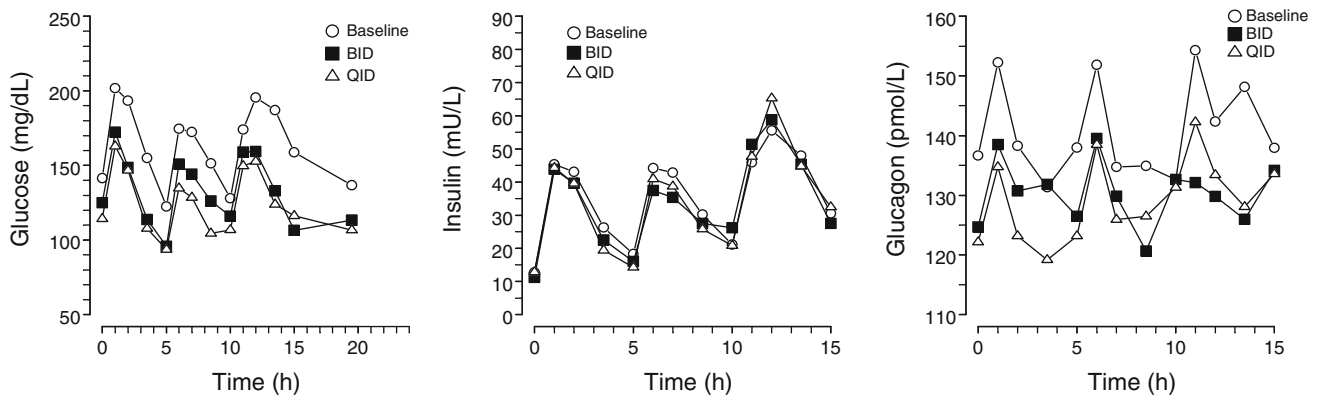

Fig. 6 Mean observed glucose, insulin, and glucagon profiles for Part C. Baseline and the last day of the treatment period (study days 13 and 26) for subjects with T2DM administered LY2599506 on a BID or QID schedule

Overall, insulin concentrations were not significantly greater during treatment with LY2599506, but glucose-normalized insulin concentrations were increased by LY2599506 [21, 22]. This observation is consistent with augmentation of insulin secretion with respect to the ambient glucose concentration, as expected for a glucokinase activator. The physiological circadian rhythm for endogenous insulin secretion in the model aided in a better

understanding of the onset, offset, and magnitude of drug effect, in spite of the absence of extensive nocturnal insulin sampling during the study [4].

LY2599506 produced dose-dependent hypoglycemia as expected in this dose-escalation study. Hypoglycemia occurred primarily in late post-prandial time periods, between 2 and 5 h after dosing with the previous meal. Subjects who were most sensitive to glucose lowering

Table 2 Assessment of the effect of LY2599506 on glucose and insulin

Drug Effect Model	OFV change[a]
LY2599506 on pancreatic insulin secretion	−505
LY2599506 on hepatic glucose production	−124
LY2599506 on pancreatic insulin secretion and on hepatic glucose production	−581

OFV objective function value

[a] The OFV of the reference model = 39420

Table 3 Parameter estimates for glucose, insulin, and glucagon dynamics

| Parameter	Unit	Typical value	IIV (%)	Median (5–95th percentile)
Glucose central volume of distribution (V_G)	L	9.33	30	–
Glucose peripheral volume of distribution (V_P)	L	8.56	10	–
Insulin-independent glucose clearance (CL_G)	L/min	0.0287	65	–
Insulin-dependent glucose clearance (CL_{GI})	(L/min)/(mU/L)	0.00548	40	0.00492 (0.00413–0.00584)
Inter-compartmental glucose clearance (Q)	L/min	0.442	104	–
Glucose effect compartment rate constant (k_{GE})	1/min	0.1016	21	–
Glucose bioavailability (*BIOG*)	–	1.1	–	–
Glucose and protein absorption rate constant (k_{abs})	1/min	0.0109	–	0.0109 (0.0102–0.0116)
Steady-state glucose concentration (G_{SS})	mg/dL	146	20	146 (137–158)
Glucagon effect on glucose production (*GPRG*)	–	0.79	–	0.836 (0.631–1.40)
Insulin volume of distribution (V_I)	L	6.09	42	–
Insulin clearance (CL_I)	L/min	1.22	30	–
Insulin effect compartment rate constant (k_{IE})	1/min	0.005685	31	–
Glucose effect on insulin production (*IPRG*)	–	1.42	36	–
Incretin effect (*SINCR*)	1/mg	0.000994	52	–
Modulation amplitude on baseline insulin secretion (*MA*)	%	−24	–	–
Modulation width on baseline insulin secretion (*MW*)	min	138	–	–
Time of maximal modulation of insulin secretion (*MTmax*)	–	18.7 h;1:10 a.m.	–	–
Steady-state insulin concentration (I_{SS})	mU/L	10.6	45	10.7 (9.26–12.3)
Glucagon volume of distribution (V_{GN})	L	28.0	–	21.7 (20.0–43.9)
Glucagon clearance (CL_{GN})	L/min	1.16	–	2.27 (0.0438 – 7.26)
Glucose effect on glucagon production (*NPRG*)	–	0.0303	–	0.0349 (0.00809–0.0625)
Slope for effect of protein on glucagon production (*GSLP*)	1/gm	0.00560	–	0.00616 (0.00407–0.0147)
Insulin effect on glucagon production (*NPRI*)	–	0.0349	–	0.0228 (0.013–0.112)
Glucagon effect compartment rate constant (k_{NE})	1/min	0.118	–	0.172 (0.0142–0.548)
Steady-state glucagon concentration (GN_{SS})	pg/mL	136	15	135 (128–143)
LY2599506 effect compartment rate constant for insulin (k_{EI})	1/min	0.00169	–	0.00155 (0.00100–0.00264)
LY2599506 effect on insulin secretion (*DIPR*)	–	0.00623	–	0.00618 (0.00534–0.00726)
LY2599506 effect compartment rate constant for glucose (k_{E2})	1/min	0.00963	–	0.021 (0.00771–0.0376)
LY2599506 effect on glucose production (*DGPR*)	–	0.0329	–	0.0359 (0.0234–0.0561)
Glucose residual error (*RESG*)	%	42	–	44 (43 – 45)
Insulin residual error (*RESI*)	%	58	–	64 (62–65)
Glucagon residual error (*RESN*)	%	35	–	36 (35–37)
Correlation (V_G–Q)	–	-0.75	–	–
Correlation (V_G–V_I)	–	0.71	–	–
Correlation (Q–V_I)	–	-0.35	–	–

IIV inter-individual variability

Estimated parameters are in bold; all other parameters are fixed to values from Jauslin et al. [4]. Dashes mean parameters were not estimated

effects of LY2599506 underwent dose reduction, while those least sensitive to LY2599506 proceeded in dose escalation. For this reason, the true dose-dependency of LY2599506-induced hypoglycemia is likely to be greater than that observed in this study. In Part B, where the dose adjustment threshold for glucose was <60 mg/dL, the

Fig. 7 Diagnostic plots of glucose, insulin, and glucagon. *Left*: individual predicted values versus observed data. *Right*: individual weighted residuals versus predicted values
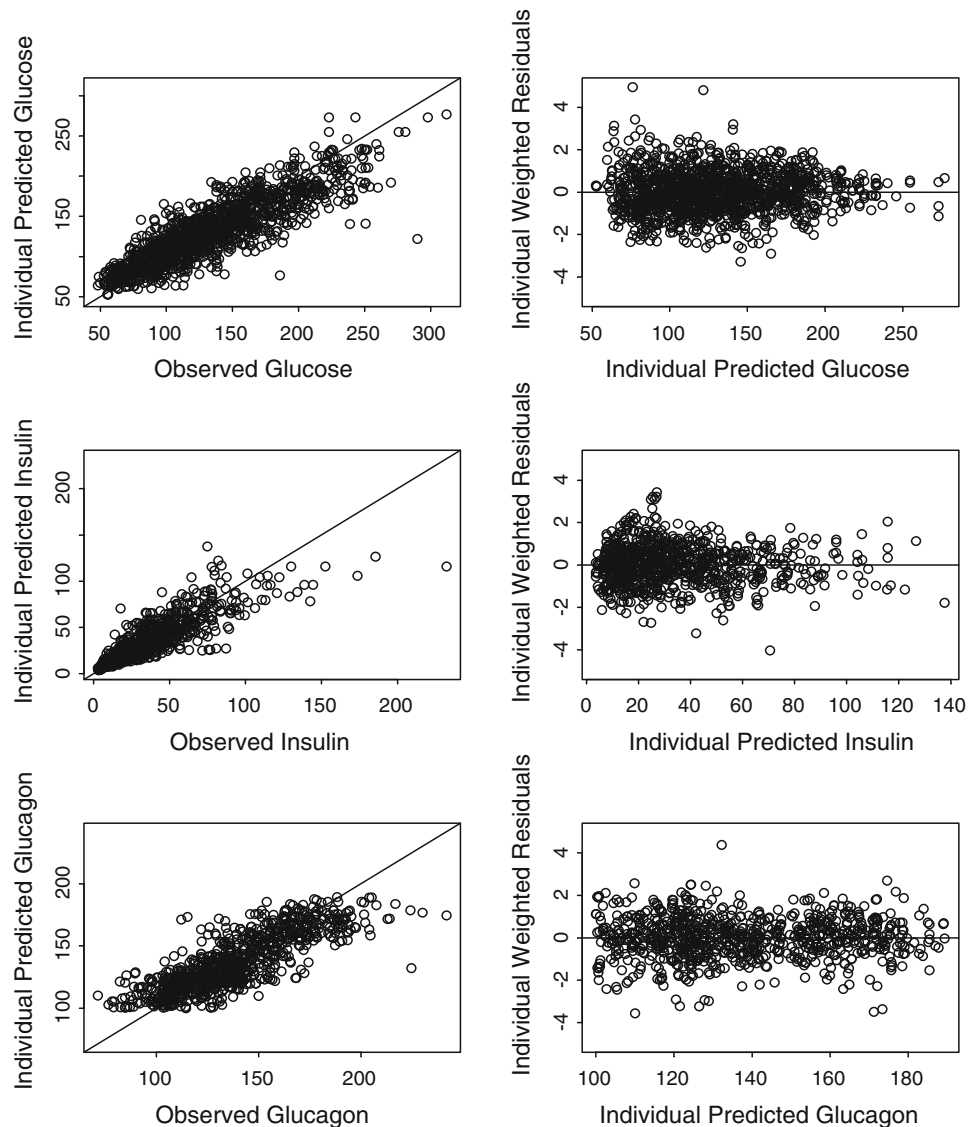
maximum tolerated total daily dose ranged from 50 to 1100 mg/day; in Part C where the dose adjustment threshold for glucose was <80 mg/dL, the total daily dose ranged from 60–530 mg/day in the QID treatment arm. The highest plasma LY2599506 concentrations were observed at bedtime when the smallest meal of the day was administered (that is, ∼200 kcal snack). Despite this, the subjects tolerated bedtime doses that were similar to other times of day. These observations suggest that LY2599506 is well-tolerated throughout a 24-hour dosing period, including the night.

Adding a glucagon and a PK component to an established integrated glucose-insulin model allowed for the analysis of data from study participants with several contributing factors affecting the glucose response, especially with the intent of understanding the anticipated incidence of hypoglycemia. It is likely that the description of glucagon dynamics represented by the present glucagon structure in the model is basic

and ignores many additional signaling pathways that contribute to the regulation of glucagon [17, 18, 23]. However, the results of the predictive check suggest that key influences on glucagon regulation are reasonably captured in the model. Combining the impact of glucose, insulin, and glucagon concentrations jointly on hepatic glucose production is conceptually similar to published studies suggesting that glucagon potency is dependent on concurrent glucose and insulin concentrations [17, 18, 23]. The shifting potency of glucagon on hepatic glucose production in fluctuating conditions of glucose and insulin concentrations has been studied extensively in both animals and humans [17, 18, 23]. In circumstances of low insulin and low glucose, glucagon was predicted by the model to increase hepatic glucose production by at least threefold (Fig. 2), a rise that is in alignment with published data [17]. To refine the glucagon model component, it may be useful to incorporate the data from both healthy subjects and subjects with T2DM from
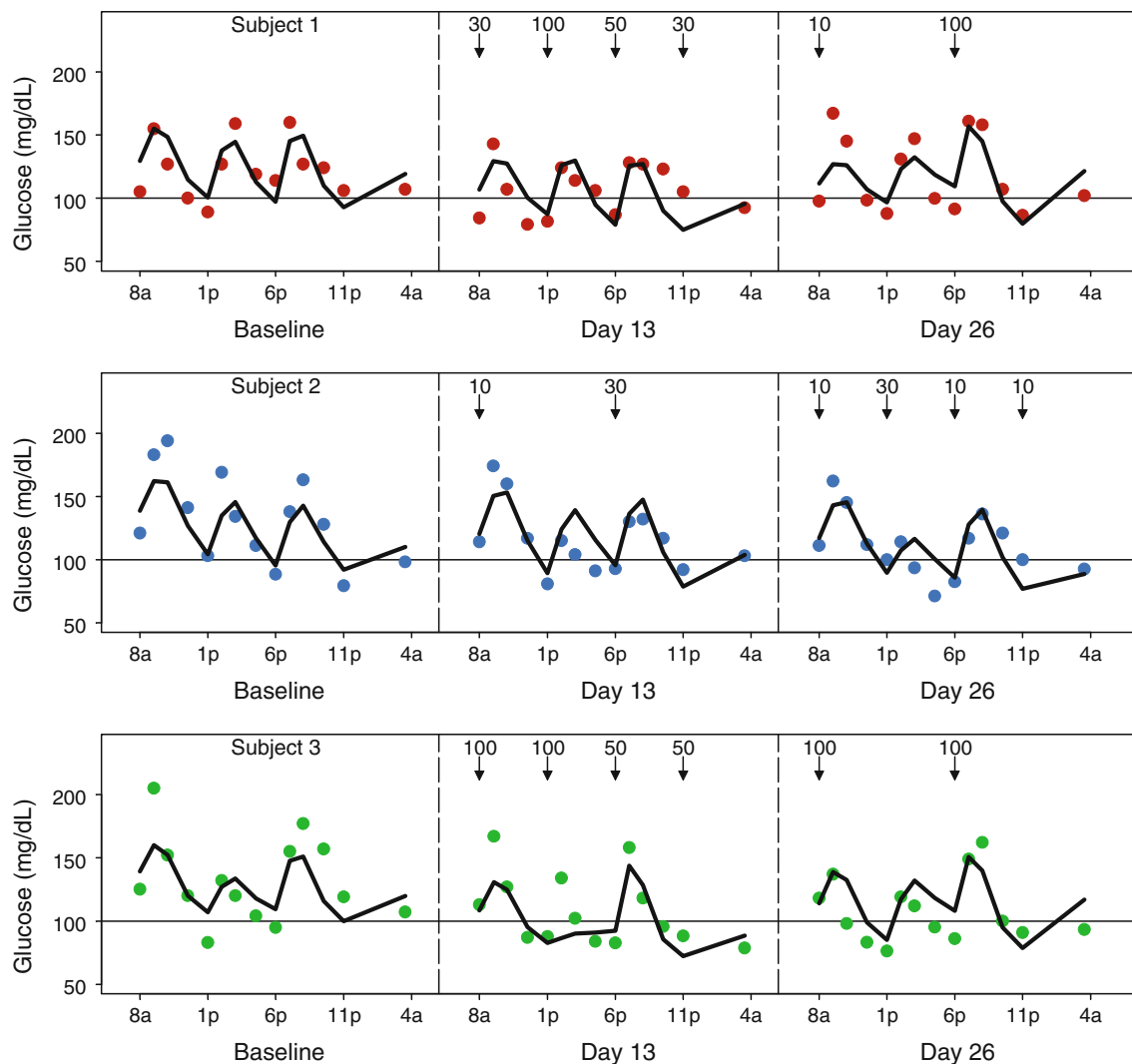
Fig. 8 Representative profiles for 3 subjects with T2DM in Part C at baseline and with LY2599506 (study days 13 and 26). Observations from the original data set are plotted as points. The *lines* show the model predicted response. *Arrows* are labeled with the administered BID or QID LY2599506 dose amounts in mg. Meals were provided during the day (8 am, 1 pm and 6 pm) and a snack given at bedtime (11 pm)

other studies to further investigate the dynamics of glucagon and to ascertain a better understanding of the variability of the physiological parameters for glucagon.

The inclusion of a drug effect on pancreatic insulin secretion produced a much greater effect on the model fit than the inclusion of a drug effect on hepatic glucose production. The model represents a simplification of actual physiology and thus, it is unlikely to discriminate between the direct effects of LY2599506 on hepatic glucose production and the suppression of hepatic glucose production secondary to insulin secretion stimulated by LY2599506. However, the more evident effect of LY2599506 on insulin secretion in the model is consistent with literature from animal models suggesting that glucokinase may be more active in β-cells in the pancreas, in contrast to hepatic glucokinase and thus, the pancreatic glucokinase may yield a more detectable response

when affected [5, 24, 25]. An intriguing path of future development would be to improve the linkage of this model to non-clinical pharmacology and mechanistic studies and include more specific details describing the means by which the drug affects the liver and pancreas.

Assessment of glucose, insulin, and glucagon data was restricted to subjects with T2DM since the majority of data from this study was from subjects with T2DM and also physiological-based parameters are expected to differ between healthy subjects and subjects with T2DM [2]. Using fixed values based on literature for the physiological based parameters for subjects with T2DM reduced the computational time required by the model by decreasing the number of parameters to be estimated. Experience with the current modeling approach suggests that the continual expansion of technology for computation may greatly aid in

the advancement of the semi-mechanistic modeling approach. Initial efforts towards modeling employed the first order condition estimation method (FOCE) in NONMEM VI using a single CPU that resulted in run times up to a week long and often produced unsuccessful convergence. Implementing the model in S–ADAPT [26] decreased the run time and improved the ability to estimate parameters. The optimal approach for the analysis described here was to use the "expectation method" (Monte Carlo Importance Sampling assisted by model a posterior estimation) in NONMEM 7.2, which facilitated reasonable parameter estimation and the most efficient use of computation resources. Depending on the number of estimated parameters included in the model and the number of available parallel processing CPUs, the run time of the model was minimized to between 12 to 24 h. Along with supporting parameter estimation, NONMEM 7.2 was also used to help evaluate model performance by applying the method of Markov Chain Monte Carlo Bayesian Analysis (BAYES) [15].

The established integrated glucose-insulin model [1–5] has proven to be adaptable, which makes it a valuable tool in anti-hyperglycemic drug development. The integrated glucose-insulin model could be customized to work with oral or intravascular routes of drug administration, to aid in the characterization of drug mechanism of action of drug, and to evaluate the effects of combination drug therapy. Including the glucagon component with the integrated glucose-insulin model may support the development of drugs that directly affect glucagon secretion from pancreatic α-cells. The model developed in this study was used to describe LY2599506, glucose, insulin, and glucagon concentrations and has the potential to advance the development of LY2599506 by producing simulations to guide the design of dose regimens for larger clinical studies. Future opportunities for model enhancement may also include linkage to a model that is able to assess drug effects, such as HbA1c changes, that develop gradually over longer time periods [27].

Appendix

Glucose submodel equations

$$\frac{dG_A}{dt} = -G_A(t) \cdot k_a \tag{12}$$

$$\frac{dG_C}{dt} = k_a \cdot G_A(t) + G_{PROD}(t) + \frac{Q}{V_P} \cdot G_P(t) - (CL_G + CL_{GI} \cdot I_E(t) + Q) \cdot \frac{G_C(t)}{V_G},$$

$$G_C(0) = G_{SS} \cdot V_G \tag{13}$$

$$\frac{dG_P}{dt} = Q \cdot \left(\frac{G_C(t)}{V_G} - \frac{G_P(t)}{V_P}\right), \ G_P(0) = G_{SS} \cdot V_P \tag{14}$$

$$G_{PROD}(t) = G_{PROD,0} = G_{SS} \cdot (CL_G + CL_{GI} \cdot I_{SS}) \tag{15}$$

$$\frac{dG_E}{dt} = k_{GE} \cdot \frac{G_C(t)}{V_G} - k_{GE} \cdot G_E(t), \ G_E(0) = G_{SS} \tag{16}$$

G_A is glucose in the absorption compartment, k_a is first-order absorption, G_C and G_P are the glucose in the central and peripheral compartments, G_{PROD} is endogenous glucose production, Q is intercompartmental clearance, V_G and V_P are the central and peripheral volumes of distribution, CL_{GI} is insulin-dependent clearance and CL_G is insulin-independent clearance, G_{SS} is glucose in the central compartment at steady-state, G_E is the glucose effect compartment, k_{GE} is the equilibration rate constant to and from the glucose effect compartment, I_E is the insulin effect compartment, I_{SS} is insulin concentration at steady-state.

Insulin submodel equations

$$\frac{dI}{dt} = I_{SEC}(t) - \frac{CL_I}{V_I} \cdot I(t), \ I(0) = I_{SS} \cdot V_I \tag{17}$$

$$I_{SEC,o} = I_{SS} \cdot CL_I \tag{18}$$

$$G_{CM}(t) = \left(\frac{G_E(t)}{G_{SS}}\right)^{IPRG} \tag{19}$$

$$I_{ABSG}(t) = 1 + S_{incr} \cdot G_A(t) \tag{20}$$

$$I_{SEC}(t) = I_{SEC,o} \cdot G_{CM}(t) \cdot I_{ABSG}(t) \tag{21}$$

$$\frac{dI_E}{dt} = k_{IE} \cdot \frac{I(t)}{V_I} - k_{IE} \cdot I_E(t), \ I_E(0) = I_{SS} \tag{22}$$

I_{SEC} is endogenous insulin secretion, CL_I is insulin clearance, V_I is the volume of distribution of insulin, $I_{SEC,0}$ is baseline insulin secretion, G_{CM} is the fraction of insulin secretion regulated by the glucose concentration in the effect compartment, $IPRG$ is the estimated power in the relationship, I_{ABSG} is the fraction of insulin secretion triggered by the incretin effect following glucose absorption from the gut, S_{incr} is the slope of a linear relationship, k_{IE} is the equilibration rate constant to and from the insulin effect compartment.

References

1. Jauslin PM, Silber HE, Frey N, Gieschke R, Simonsson US, Jorga K, Karlsson MO (2007) An integrated glucose-insulin model to describe oral glucose tolerance test data in type 2 diabetics. J Clin Pharmacol 47(10):1244–1255

2. Silber HE, Jauslin PM, Frey N, Gieschke R, Simonsson US, Karlsson MO (2007) An integrated model for glucose and insulin regulation in healthy volunteers and type 2 diabetic patients following intravenous glucose provocations. J Clin Pharmacol 47(9):1159–1171

3. Silber HE, Jauslin PM, Frey N, Karlsson MO (2010) An integrated model for the glucose-insulin system. Basic Clin Pharmacol Toxicol 106(3):189–194

4. Jauslin PM, Frey N, Karlsson MO (2011) Modeling of 24-hour glucose and insulin profiles of patients with type 2 diabetes. J Clin Pharmacol 51(2):153–164

5. Jauslin PM, Karlsson MO, Frey N (2011) Identification of the mechanism of action of a glucokinase activator from oral glucose tolerance test data in type 2 diabetic patients based on an integrated glucose-insulin model. J Clin Pharmacol 52(12): 1861–1871

6. de Winter W, DeJongh J, Post T, Ploeger B, Urquhart R, Moules I, Eckland D, Danhof M (2006) A mechanism-based disease progression model for comparison of long-term effects of pioglitazone, metformin and gliclazide on disease processes underlying Type 2 Diabetes Mellitus. J Pharmacokinet Pharmacodyn 33(3):313–343

7. Landersdorfer CB, Jusko WJ (2008) Pharmacokinetic/pharmacodynamic modelling in diabetes mellitus. Clin Pharmacokinet 47(7):417–448

8. Gao W, Jusko WJ (2012) Target-mediated pharmacokinetic and pharmacodynamic model of exendin-4 in rats, monkeys and man. Drug Metab Dispos 40(5):990–997

9. Landersdorfer CB, He YL, Jusko WJ (2012) Mechanism-based population modelling of the effects of vildagliptin on GLP-1, glucose and insulin in patients with type 2 diabetes. Br J Clin Pharmacol 73(3):373–390

10. Dahl SG, Aarons L, Gundert-Remy U, Karlsson MO, Schneider YJ, Steimer JL, Troconiz IF (2010) Incorporating physiological and biochemical mechanisms into pharmacokinetic-pharmacodynamic models: a conceptual framework. Basic Clin Pharmacol Toxicol 106(1):2–12

11. Matschinsky FM (2009) Assessing the potential of glucokinase activators in diabetes therapy. Nat Rev Drug Discov 8(5): 399–416

12. Zhang L, Beal SL, Sheiner LB (2003) Simultaneous vs. sequential analysis for population PK/PD data I: best-case performance. J Pharmacokinet Pharmacodyn 30(6):387–404

13. Zhang L, Beal SL, Sheinerz LB (2003) Simultaneous vs. sequential analysis for population PK/PD data II: robustness of methods. J Pharmacokinet Pharmacodyn 30(6):405–416

14. Sharma A, Jusko WJ (1998) Characteristics of indirect pharmacodynamic models and applications to clinical drug responses. Br J Clin Pharmacol 45(3):229–239

15. Bauer R (2011) NONMEM User's guide, introduction to NONMEM 7.2.0. ICON Development solutions, Ellicott City, MD

16. Yano Y, Beal SL, Sheiner LB (2001) Evaluating pharmacokinetic/pharmacodynamic models using the posterior predictive check. J Pharmacokinet Pharmacodyn 28(2):171–192

17. Cherrington AD (1999) Banting Lecture, 1997.Control of glucose uptake and release by the liver in vivo. Diabetes 48(5):1198–1214

18. Ramnanan CJ, Edgerton DS, Kraft G, Cherrington AD (2011) Physiologic action of glucagon on liver glucose metabolism. Diabetes Obes Metab 13(Suppl 1):118–125

19. Meyer C, Stumvoll M, Nadkarni V, Dostou J, Mitrakou A, Gerich J (1998) Abnormal renal and hepatic glucose metabolism in type 2 diabetes mellitus. J Clin Invest 102(3):619–624

20. Meyer C, Woerle HJ, Dostou JM, Welle SL, Gerich JE (2004) Abnormal renal, hepatic, and muscle glucose metabolism following glucose ingestion in type 2 diabetes. Am J Physiol Endocrinol Metab 287(6):E1049–E1056

21. Bue-Valleskey JM, Schneck KB, Sinha VP, Wondmagegnehu ET, Kapitza C, Miller JW (2011) LY2599506, a novel glucokinase activator (GKA), improves fasting and postprandial glucose in patients wtih type 2 diabetes mellitus (T2DM) [abstract]. Diabetes 60(Suppl 1):A272

22. Bue-Valleskey JM, Schneck KB, Sinha VP, Wondmagegnehu ET, Kapitza C, Miller JW (2011) LY2599506, a novel glucokinase activator (GKA), improves fasting and postprandial glucose in patients wtih Type 2 diabetes mellitus. In: 47th EASD Annual Meeting, Lisbon, 12–16 September 2011. European Association for the study of diabetes

23. Walker JN, Ramracheya R, Zhang Q, Johnson PR, Braun M, Rorsman P (2011) Regulation of glucagon secretion by glucose: paracrine, intrinsic or both? Diabetes Obes Metab 13(Suppl 1): 95–105

24. Postic C, Shiota M, Magnuson MA (2001) Cell-specific roles of glucokinase in glucose homeostasis. Recent Prog Horm Res 56:195–217

25. Postic C, Shiota M, Niswender KD, Jetton TL, Chen Y, Moates JM, Shelton KD, Lindner J, Cherrington AD, Magnuson MA (1999) Dual roles for glucokinase in glucose homeostasis as determined by liver and pancreatic beta cell-specific gene knockouts using Cre recombinase. J Biol Chem 274(1):305–315

26. Bauer R (2008) S-ADAPT/MCPEM User's Guide (version 1.56). Berkeley, CA

27. Hamren B, Bjork E, Sunzel M, Karlsson M (2008) Models for plasma glucose, HbA1c, and hemoglobin interrelationships in patients with type 2 diabetes following tesaglitazar treatment. Clin Pharmacol Ther 84(2):228–235